Structural Engineering and Mechanics, *Vol. 65, No. 6 (2018) 731-739*
DOI: https://doi.org/10.12989/sem.2018.65.6.731

Optimal stiffness distribution in preliminary design of tubed-system tall buildings

Arsalan Alavi and Reza Rahgozar*

Department of Civil Engineering, Faculty of Engineering, Shahid Bahonar University of Kerman, Kerman, Iran

(Received December 25, 2016, Revised January 15, 2018, Accepted January 17, 2018)

Abstract. This paper presents an optimal pattern for distributing stiffness along a framed tube structure through an analytic equation, which may be used during the preliminary design stage. Most studies in this field are computationally intensive and time consuming, while a hand-calculation method, as presented here, is a more suitable tool for sensitivity analyses and parametric studies. Approach in development of the analytic model is to minimize the mean compliance (external work) for a given volume of material. A variational statement of the problem is made, and a specified deformation-profile is obtained as the necessary condition for a minimum; enforcing this condition, stiffness is then computed. Due to some near-zero values for stiffness, the problem is modified by considering a lower bound constraint. To deal with this constraint, the design domain is assumed to be divided into two zones of constant stiffness and constant curvature; and the problem is restated in terms of these concepts. It will be shown that this methodology allows for easy computation of stiffness through an analytic and dimensionless equation, valid in any system of units. To show practicality of the proposed method, a tubed-system structure with uniform stiffness distribution is redesigned using the proposed model. Comparative analyses of the results reveal that in addition to simplicity of the proposed method, it provides a rather high degree of accuracy for real-world problems.

Keywords: high-rise building; framed tube; compliance; optimal stiffness

1. Introduction

Because of high cost of construction in tall buildings, optimization process is significantly important in the design stage (Aldwaik and Adeli 2014). Optimization of lateral stiffness along the height of such structures greatly affects structural responses. Generally, in most structural problems, one attempts to distribute a given volume of material within a specified region with the objective of making the structure as stiff as possible. There is no unique measure of stiffness in this process. The so-called compliance or equivalently external work measure, as is used herein, is usually selected for one crucial reason; roughly speaking, the optimization process based on this measure tends to create a system with almost uniform stress distribution (Christensen and Klarbring 2009). Connor and Laflamme (2014) introduced constant curvature as an ideal performance for a tall structure, and a formulation for lateral stiffness was proposed by enforcing this requirement. Although, they did not construct an optimization problem, they accepted a necessary condition that coincides with the general result of the compliance optimization formulation. In the current paper, this model is devised in an optimization-framework so to make the structural-improvement quantifiable. Furthermore, the formulation presented by Connor and Laflamme (2014) generates too small values for the regions near the structure's top; this problem is resolved here by observing a lower bound constraint in an analytical framework. Although such constraints have been explored by many researchers so far, most of them are numerical (Chan *et al*. 2010, Stromberg *et al*. 2011, Lee *et al*. 2012).

In general, the design process of a tall building involves conceptual design and approximate analysis, preliminary design, and finally, detailed design (Jayachandran 2009). Some engineers skip the preliminary design, which based on certain objectives, a suitable stiffness distribution can be calculated. After the conceptual design stage, they progress straight to the detailed design, and finalize the structural configuration using some type of optimization algorithm. However, this approach is more time consuming and costly. Furthermore, considering the preliminary design step allows for assessment of structural performance based on certain constraints. Although, many papers related to the preliminary step can be found, most of them are suitable for abstract analyses, but not for design (Kwan 1994, Kaviani *et al*. 2008, Rahgozar *et al*. 2011, Rahgozar and Malekinejad 2012, Jahanshahi and Rahgozar 2012). In addition, most developed methods for design are numerical. Aldwaik and Adeli (2014) presented a review of papers on optimization of high-rise structures. Almost all of the mentioned papers in that research are computer-based, while a hand-calculation method is more efficient during the early stage of design (Connor and Pouangare 1991).

In the preliminary design field, Connor and Pouangare (1991) proposed a string-shear-panel system suitable for modelling framed tube structures, and parametric relations for preliminary design are presented. Moon *et al*. (2007) and Moon (2012) developed an analytic approach for initial design of diagrid systems. In another study, Liu and Ma (2017) investigated diagrid systems with arbitrary

*Corresponding author, Professor
E-mail: rahgozar@uk.ac.ir

ISSN: 1225-4568 (Print), 1598-6217 (Online)

Fig. 1 Framed-tube system used in Dewitt Chestnut building

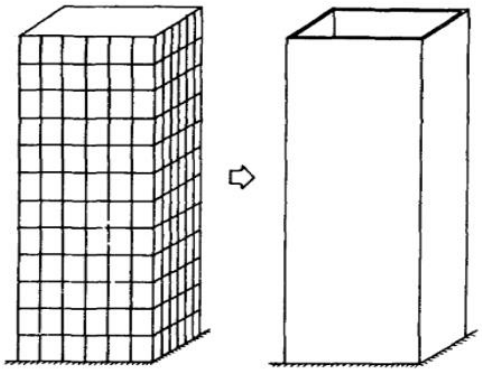

Fig. 2 Idealized model for a framed tube system (Kwan 1994)

polygonal section. In a research conducted by Montuori *et al*. (2014), strength criteria, in addition to stiffness requirements are assessed for preliminary design. A stiffness-based approach suitable for determining member sizes of braced tube structures is presented in the study by Moon (2010). The aforementioned studies are mainly stiffness-based, suitable for diagrid and braced systems. The objective of the current research is to investigate such problems, addressing the framed tube structures.

In a tubed-system structure, the induced lateral loads are resisted by axial stress field generated in the closely spaced columns located on structure's perimeter, Fig. 1.

Based on Kwan 1994 and Smith and Coull 1996, a cantilevered hollow-box-beam is a reasonable model for this system, Fig. 2.

The structure behavior is modeled as an Euler-Bernoulli beam; however, considering shear lag effect would probably better represent structure's actual response (Khan and Smith 1976, Coull and Bose 1975, Coull and Ahmed 1978, Mazinani *et al*. 2014), and is planned for future research efforts. The cross section of the equivalent

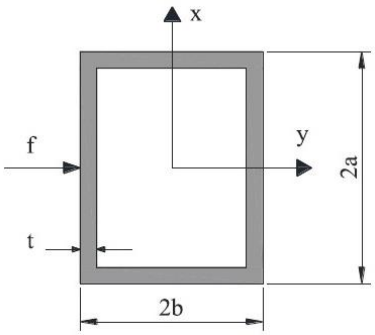

Fig. 3 Hollow box section for bending resisting system of the structure

structure is presented in Fig. 3. Thickness of the box t, which accounts for strength of the perimeter columns, is taken here as the independent variable. The optimization process applied here uses external work as the objective function. It will be shown that this selection results in constant curvature as the optimality requirement, and the thickness of the box is calculated with this objective. As to be expected, thickness value at high elevations becomes relatively small. By observing a lower bound constraint, above a certain height, defined here as the primary height (PH), the thickness values violate this limit. Dealing with this constraint in an analytic framework was a challenge in this research. To deal with this issue, the problem is restated in terms of new parameters critical curvature, and critical height (CH) with specified characteristics. It will be shown that such methodology makes the problem easy to be solved analytically.

2. Optimality criterion

In the compliance approach, the external work (compliance) is selected as the objective function to be minimized. Equivalently, total potential energy can be selected as the objective function. For the cantilever model [Fig. 2] with length h, and a coordinate system with origin at top of the structure (free end) with positive z direction pointing downward, the total potential energy is

$$J = \frac{1}{2}\int_0^h D\left(\frac{d^2u}{dz^2}\right)^2 dz - \int_0^h f(z)u\,dz \tag{1}$$

where J is the total potential energy, u denotes the lateral displacement field, and $f(z)$ is the induced lateral force. Parameter D stands for flexural stiffness. For a framed tube system which is modeled as a hollow-box-beam [Fig. 3] the flexural stiffness would be

$$D = EI \tag{2}$$

where E is Young's modulus of elasticity, and I is the moment of inertia about the x axis which is approximated as

$$I = I(z) = t(z)\,I_0 \tag{3}$$

where t is thickness of the box and $I_0 = \left[(4/3)b^3 + 4ab^2\right]$

is the moment of inertia for a unit thickness box, in which 2*a* and 2*b* are dimensions in *x* and *y* directions respectively, Fig. 3.

Based on the principle of minimum potential energy, the displacement field *u* of a system in equilibrium minimizes the total potential energy of that system; hence the following can be stated (Christensen and Klarbring 2009),

Find $u \in k$ such that

$$J(u)=\frac{1}{2}B(\mathrm{u},\mathrm{u})-C(\mathrm{u})=\min_{v\in k}J(v) \tag{4}$$

in which $B(u,u)=\int_0^h D(\frac{d^2u}{dz^2})^2dz$ is the strain energy and $C(u)=\int_0^h u f\,dz$ is the work done by external forces (compliance). Here k is the space of admissible displacement functions. For the problem at hand $k=\left\{u\in C^4[0,h]\ \text{s.t.}\ u(h)=u'(h)=0\right\}$. Minimizing *J* with respect to *v* by a suitable method, such as Gateaux derivative, ends in a new problem (Christensen and Klarbring 2009),

Find $u \in k$ such that

$$\underset{v\in k}{B(u,v)=C(v)} \tag{5}$$

which is well known as principle of virtual work. Since $B(u,v)=C(v)$ is satisfied for all $v \in k$, it also holds true for *u* in particular. Thus, the state of equilibrium would be (Bendsøe and Sigmund 2003, Christensen and Klarbring 2009)

$$B(u,u)=C(u) \tag{6}$$

The problem of design with *t* as the independent variable can be stated as an optimization problem with a proper objective function. The most common objective function in structural problems is the external work, *C*(*u*). The goal of such problems is to find *t* such that it will minimize *C*(*u*) (Bendsøe and Sigmund 2003, Christensen and Klarbring 2009). From Eqs. (4) and (6)

$$C(u_t)=-2J(u_t)=-2\min_{v\in k}J(v,t) \tag{7}$$

Based on Eq. (7), *C* and *J* are proportional, so *J* can be selected as the objective function instead of *C*. However, due to the negative sign, the minimization statement must be converted to a maximization one. In preceding relations, subscript *t* emphasizes that *u* is a function of *t*, so $J(u_t)$ can be replaced by *J*(*t*). Therefore, the design problem can be stated as follows,

$$\begin{aligned}&\underset{t}{\text{maximize}} \quad J(t)\\ &\text{Subject to } \int_0^h t\,dz=A\end{aligned} \tag{8}$$

In this formulation, *t* is selected as the only independent variable and its total amount is constrained by upper bound *A*. It should be noted that, the minimization of *J* in Eq. (4) is an equilibrium requirement for a known *t*, whereas in the maximization problem (8), *t* must be determined as the independent variable.

The Lagrangian method is adopted to solve the optimization problem (8). Substituting Eqs. (2) and (3) into Eq. (1) results in $J=0.5EI_0\int_0^h t(d^2u/dz^2)^2dz-\int_0^h f(z)u\,dz$ for which a Lagrangian functional can be taken in the form,

$$\mathrm{L}(t,\lambda)=J(t)-\lambda\left[\int_0^h t\,dz-A\right] \tag{9}$$

where $\lambda \geq 0$ is the Lagrangian multiplier. By use of calculus of variation method, the optimality condition of $\delta\mathrm{L}=0$ with respect to *t* yields

$$\frac{d^2u}{dz^2}=\pm(\frac{2\lambda}{EI_0})^{1/2}=\pm\kappa \tag{10}$$

where κ denotes the curvature. According to Eq. (10), at the optimal state, the absolute value of the curvature should be constant along the structure, which is in agreement with the general theorem of constant strain energy presented by Christensen and Klarbring (2009). More simply, the constant-curvature should be taken as the optimality criterion in this method. Therefore, the stiffness would be determined with the requirement of producing this specified deformation profile.

2.1 Optimal thickness design

In this section different loading patterns of concentrated, uniform, triangular and quadratic are considered, and for each case, optimal thickness distribution is obtained. For all cases, general form of the governing equation, along with natural boundary condition (NBC) are presented

$$\begin{aligned}&\text{for } 0\le z\le h && \frac{d^2}{dz^2}[D\frac{d^2u}{dz^2}]=f\\ &NBC:\text{ for } z=0 && \begin{cases}\frac{d}{dz}[D\frac{d^2u}{dz^2}]=S\\ [D\frac{d^2u}{dz^2}]=B\end{cases}\end{aligned} \tag{11}$$

where, induced lateral load (*f*) and NBC, including the shear force (*S*) and the bending moment (*B*) at the free end, is defined for each case in Table 1. *Q* and *q* in Table 1 denote the concentrated load and the maximum intensity of distributed load, respectively, both at top of the structure. The dimensionless parameter $\bar{z}=z/h$ is used for convenience.

Table 1 Loading pattern and natural boundary condition

	f	*S*	*B*
Concentrated	0	*Q*	0
Uniform	*q*	0	0
Triangular	$q(1-\bar{z})$	0	0
Quadratic	$q(1-\bar{z}^2)$	0	0

Table 2 M and m for different cases

	M	m
Concentrated	Qh	$\bar{z}$
Uniform	$(1/2)qh^2$	$\bar{z}^2$
Triangular	$(1/3)\,qh^2$	$-(1/2)\bar{z}^3+(3/2)\bar{z}^2$
Quadratic	$(5/12)qh^2$	$-(1/5)\bar{z}^4+(6/5)\bar{z}^2$

The variable t required to produce the preselected performance presented by Eq. (10) should be evaluated. To that end, the governing differential Eq. (11) would be considered; integrating it twice and taking NBC into account contributes to

$$D\frac{d^2u}{dz^2}=M\ m(\bar{z}) \tag{12}$$

where M is maximum moment that happens at the base, and we name $m(\bar{z})$ relative moment that depends on $\bar{z}$. Table 2 presents these two parameters for each case.

Clearly, $M, D \geq 0$ for all $\bar{z} \in [0\ \ 1]$. According to equations of $m(\bar{z})$ from Table 2, $m(\bar{z}) \geq 0$ for all $\bar{z} \in [0\ \ 1]$. Therefore, it is concluded from Eq. (12) that $d^2u/dz^2 \geq 0$. Hence, by Eq. (10)

$$\frac{d^2u}{dz^2}=+\kappa \tag{13}$$

Substituting for D, I and d^2u/dz^2 from Eqs. (2), (3) and (13) respectively into Eq. (12), and defining new parameter $\kappa_0 = M/EI_0$, which is the maximum curvature in a unit thickness box (that happens at the base level), results in

$$t\kappa=\kappa_0 m(\bar{z}) \tag{14}$$

Thus, considering κ as a constant parameter, optimal thickness value would be

$$t(\bar{z})=\frac{\kappa_0}{\kappa}m(\bar{z}) \tag{15}$$

Indeed, this formulation must satisfy presented constraint in formulation (8), but it is required to restate this constraint with respect to the new variable $\bar{z}$ in advance, as is done in the following,

$$\int_0^1 t\,d\bar{z}=\bar{t} \tag{16}$$

where

$$\bar{t}=\frac{A}{h} \tag{17}$$

This is the limited volume (LV) constraint. $\bar{t}$ is defined for convenience and is named as average thickness. Substituting Eq. (15) into constraint (16) dictates the value of κ, which after substitution in Eq. (15), the optimal thickness relations are obtained, Table 3.

Table 3 Optimal thickness, observing LV constraint

Concentrated	$2\bar{t}\,\bar{z}$
Uniform	$3\bar{t}\,\bar{z}^2$
Triangular	$-(4/3)\bar{t}\,\bar{z}^3+4\bar{t}\,\bar{z}^2$
Quadratic	$-(5/9)\bar{t}\,\bar{z}^4+(10/3)\bar{t}\,\bar{z}^2$

Table 4 Polynomials associate with PH

Concentrated	$2\bar{z}_p-\bar{t}_{\min}=0$
Uniform	$3\bar{z}_p^2-\bar{t}_{\min}=0$
Triangular	$-(4/3)\bar{z}_p^3+4\bar{z}_p^2-\bar{t}_{\min}=0$
Quadratic	$-(5/9)\bar{z}_p^4+(10/3)\bar{z}_p^2-\bar{t}_{\min}=0$

3. Treating a lower bound constraint on the thickness

The presented equations in Table 3 yield near-zero values for some points, almost located at the top of the structure. To avoid this practical problem, the lower bound constraint $0<t_{min}\leq t$ should be observed. Therefore, the new optimization problem would be stated as

$$\begin{aligned} &\underset{t}{\text{maximize}} && J(t)\\ &\text{Subject to} && \begin{cases}\text{LV}: \int_0^1 t\,d\bar{z}=\bar{t}\\ \text{LB}: 0<t_{min}\leq t\end{cases}\end{aligned} \tag{18}$$

where LV and LB stand for limited volume and lower bound constraints, respectively.

From Table 3, LB constraint is not satisfied for some $\bar{z}$. Clearly, there exists a height named primary height (PH), denoted by $\bar{z}_p$ in dimensionless relations, such that for $\bar{z} \in [0\ \ \bar{z}_p]$, LB constraint is violated. Referring to Table 3, PH can be calculated by substituting $\bar{z}_p$ for $\bar{z}$ and $t_{\min}$ for t. Doing so and introducing a parameter named relative minimum thickness (RMT) as

$$\bar{t}_{\min}=\frac{t_{\min}}{\bar{t}} \tag{19}$$

yields polynomials for which an acceptable root would be considered as the PH value. Table 4 presents the relevant polynomials for each case. It should be noted that $t_{\min}$ is always lower than $\bar{t}$, otherwise LV constraint is violated. Therefore, $\bar{t}_{\min} \in [0\ 1]$.

At the first glance, it may seem that to treat LB

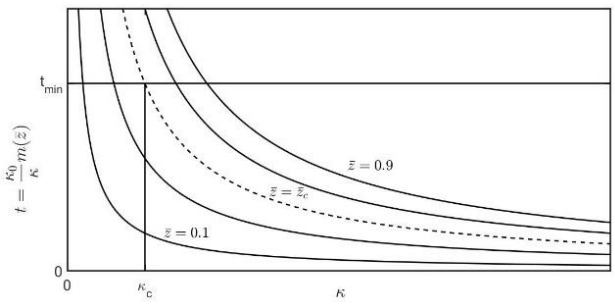

Fig. 4 Variation of t with respect to κ for different values of $\bar{z}$

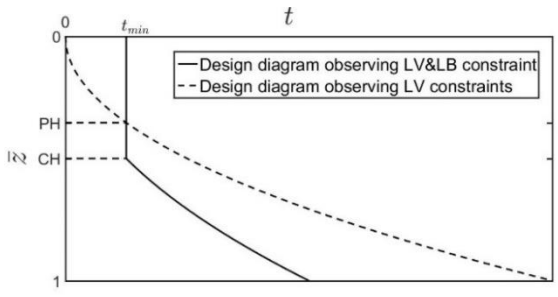

Fig. 5 Illustration for CH and PH

constraint, the points above PH ($\bar{z} \in [0 \quad \bar{z}_p]$) should have t_{min} and the thicknesses of the lower points ($\bar{z} \in [\bar{z}_p \quad 1]$), evaluated from Table 3, must be modified to satisfy LV constraint. However, this is not true in general, and it needs more detailed investigation, which is done in the following subsection.

3.1 Method of solution

There are some approaches to deal with the new optimization problem which includes LB constraint. Some authors assign a Lagrangian multiplier to LB and treat it as an inequality constraint. However, it is more reasonable to treat LB constraint separately as is done here. In this approach, a Lagrangian function is constructed using the objective function and LV constraint while ignoring LB constraint. Lagrangian function is then minimized (or maximized) with respect to LB constraint. This process results in a relation between the Lagrangian multiplier λ and the independent variable t through a one-variable function $\varphi(\lambda)$

$$\varphi(\lambda) = \min_{t \in LB} \mathrm{L}(t, \lambda) \tag{20}$$

Finally, due to convexity of the problem (Christensen and Klarbring 2009), the optimum solution is obtained by maximizing (or minimizing) $\varphi(\lambda)$ with respect to $\lambda \geq 0$

$$\begin{cases} \max\limits_{\lambda} \varphi(\lambda) \\ s.t.\ \lambda \geq 0 \end{cases} \tag{21}$$

Consequently, it is essential to find the relation between λ and t at the first step and construct a relation in the form of Eq. (20). However, this process is rather complicated and a simpler approach is take here. To deal with this complexity, this research strives to construct a relation between t and an intervening variable, instead of λ. According to monotonic relation of κ and λ by Eq. (10), κ seems to be suitable as the intervening variable. Appropriateness of this selection is supported by two factors: 1) the problem is extremely simplified as compared to the λ formulation. 2) the results are more sensible from a structural viewpoint, because the intervening variable is the structure's curvature.

According to Eq. (15), and the fact that κ_0 and $m(\bar{z})$ are positive in the design domain [0 1] for all loading patterns, function of t with respect to κ in different elevations of $\bar{z}$ would be in the form of presented in Fig. 4, with the marked position of minimum thickness t_{min} and the particular unknown κ_c which denotes the structure curvature at the optimum state. Considering Fig. 4, there is a critical height (CH), $\bar{z}_c$ located on the chart at intersection of $t = t_{\min}$ and $\kappa = \kappa_c$. At elevations higher than the CH value ($0 \leq \bar{z} \leq \bar{z}_c$) LB constraint is violated; hence for this region, uniform thicknesses (t_{min}) with varying curvature, as computed from Eq. (14) is considered. We call this region constant thickness (CT) zone, formally specified as,

$$\mathrm{CT}(0 \leq \bar{z} \leq \bar{z}_c): \begin{cases} t_{CT} = t_{min} \\ \kappa_{CT} = \dfrac{\kappa_0}{t_{\min}} m(\bar{z}) \end{cases} \tag{22}$$

For heights lower than CH ($\bar{z}_c \leq \bar{z} \leq 1$), curvature is kept constant at κ_c with varying thickness computed from Eq. (14). This region is referred to as the constant curvature (CC) zone with following specifications

$$\mathrm{CC}(\bar{z}_c \leq \bar{z} \leq 1): \begin{cases} t_{CC} = \dfrac{\kappa_0}{\kappa_c} m(\bar{z}) \\ \kappa_{CC} = \kappa_c \end{cases} \tag{23}$$

Note that CH and PH are different in general. Indeed, PH is related to LV optimization problems, whereas CH is related to LV-LB ones. Fig. 5 clarifies the difference between CH and PH.

3.2 Modified optimal thickness and curvature distribution

In the presented formulations for CC and CT zones, there are two unknowns $\bar{z}_c$ and κ_c that should be determined. On the other hand, there are two constraints to be satisfied. First, it should be noted that the thickness must remain continuous along the structure's height. Thus, from Eqs. (22) and (23) $t_{CT}(\bar{z}_c) = t_{CC}(\bar{z}_c)$, that satisfying this relation

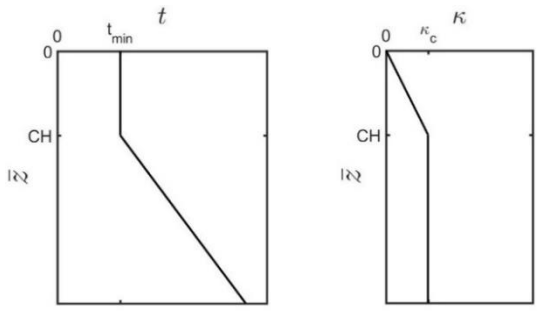

Fig. 6 Diagrams of thickness (t) and curvature (κ) in optimal state for concentrated load case

Table 5 Polynomials associate with CH

Concentrated	$\bar{t}_{\min}\bar{z}_c^2 - 2\bar{z}_c + \bar{t}_{\min} = 0$
Uniform	$2\bar{t}_{\min}\bar{z}_c^3 - 3\bar{z}_c^2 + \bar{t}_{\min} = 0$
Triangular	$3\bar{t}_{\min}\bar{z}_c^4 - (8\bar{t}_{\min} + 4)\bar{z}_c^3 + 12\bar{z}_c^2 - 3\bar{t}_{\min} = 0$
Quadratic	$4\bar{t}_{\min}\bar{z}_c^5 - 5\bar{z}_c^4 - 20\bar{t}_{\min}\bar{z}_c^3 + 30\bar{z}_c^2 - 9\bar{t}_{\min} = 0$

yields the following term for κ_c,

$$\kappa_c = \frac{\kappa_0}{t_{min}} m(\bar{z}_c) \tag{24}$$

Substituting the obtained equation of κ_c into Eqs. (22) and (23) results in the following relations for thickness and curvature; for thickness

$$t(\bar{z}) = \begin{cases} t_{min} & 0 \le \bar{z} \le \bar{z}_c \\ t_{min}\dfrac{m(\bar{z})}{m(\bar{z}_c)} & \bar{z}_c \le \bar{z} \le 1 \end{cases} \tag{25}$$

and for curvature

$$\kappa(\bar{z}) = \begin{cases} \dfrac{\kappa_0}{t_{\min}} m(\bar{z}) & 0 \le \bar{z} \le \bar{z}_c \\ \dfrac{\kappa_0}{t_{min}} m(\bar{z}_c) & \bar{z}_c \le \bar{z} \le 1 \end{cases} \tag{26}$$

For illustration, Fig. 6 displays diagrams of $t(\bar{z})$ and $\kappa(\bar{z})$ for concentrated load case, in which $m(\bar{z}) = \bar{z}$. Similar diagrams can be generated for other loading patterns.

Second, LV constraint, presented in Eq. (16), must be imposed to obtain $\bar{z}_c$. By substituting the computed thickness from Eq. (25) into Eq. (16), a polynomial with a root acceptable as the CH value is obtained. Applying to all cases results in the relations presented in Table 5.

Solving the equations presented in Table 5 while observing $0 \le \bar{z}_c \le 1$ and $0 \le \bar{t}_{min} \le 1$ would yield $\bar{z}_c$ (CH). For different discrete values of RMT ($\bar{t}_{min} = 0, 0.1, ..., 0.9$), CH is calculated based on Table 5. Then, by help of a curve fitting method, the closed-form equation of CH in terms of RMT is obtained and the results are presented in Table 6.

Table 6 CH equation in terms of RMT

Concentrated	$4.505\bar{t}_{min}^{\,4} - 7.0374\bar{t}_{min}^{\,3} + 3.5502\bar{t}_{min}^{\,2} - 0.045\bar{t}_{min} + 0.0095$
Uniform	$1.2529\bar{t}_{min}^{\,4} - 0.2699\bar{t}_{min}^{\,3} - 1.5707\bar{t}_{min}^{\,2} + 1.557\bar{t}_{min} + 0.0142$
Triangular	$1.9394\bar{t}_{min}^{\,4} - 1.5852\bar{t}_{min}^{\,3} - 0.6734\bar{t}_{min}^{\,2} + 1.2873\bar{t}_{min} + 0.0141$
Quadratic	$1.6515\bar{t}_{min}^{\,4} - 0.9985\bar{t}_{min}^{\,3} - 1.1081\bar{t}_{min}^{\,2} + 1.4231\bar{t}_{min} + 0.0145$

Table 7 PH equation in terms of RMT

Concentrated	$0.5\bar{t}_{min}$
Uniform	$0.5773\bar{t}_{min}^{\,0.5}$
Triangular	$-1.6774\bar{t}_{min}^{\,4} + 4.104\bar{t}_{min}^{\,3} - 3.6074\bar{t}_{min}^{\,2} + 1.7246\bar{t}_{min} + 0.0065$
Quadratic	$-1.8342\bar{t}_{min}^{\,4} + 4.4881\bar{t}_{min}^{\,3} - 3.9462\bar{t}_{min}^{\,2} + 1.8442\bar{t}_{min} + 0.0071$

By a similar approach and using Table 4, PH values can be obtained also in terms of RMT. The result of such calculation is presented in Table 7. Comparing the Table 6 and 7 reveals that the CH and PH values are not identical.

4. Illustrative example

The proposed method is applied to a tall building for illustration. The example given by Kwan (1994) is selected as the basic model, which is a framed tube structure with uniform stiffness distribution subjected to a uniform loading. This structure will be redesigned (with identical amount of material) using the proposed method. The models are then analyzed by means of a standard program, and the results are graphically compared.

4.1 Structural details

The reference structure is a 40-story reinforced concrete framed tube building with typical height story of 3 m. All columns and beams have the size of $80cm \times 80cm$ with center-to-center spacing of 2.5 m. Equivalent properties of the orthotropic membrane tube model of this structure are presented as followings

$$\begin{aligned} &q = 120kN/m \quad E = 20GPa \quad h = 120m \\ &a = 17.5m \quad b = 15m \quad t = 25.6cm \end{aligned} \tag{27}$$

where a, b, h and t are geometric characteristics based on Fig. 3; E is the modulus of elasticity; and q is the uniform load

intensity.

Redesign of this structure based on the presented relations, requires two more parameters $\bar{t}$ and $t_{\min}$. As thickness in the first structure is uniformly distributed, its value is equal to the average thickness, or $\bar{t} = 25.6cm$.

Cross sectional dimension of $50cm \times 50cm$ is supposed as the accepted minimum size for columns. Using the relation $t = A_c / s$ (Kwan 1994), in which A_c is columns' cross sectional area and *s* is the column spacing, which is 2.5*m* here, the minimum thickness for the equivalent tube model would be $t_{\min} = 10cm$.

4.2 Structural design

As the first input, $\bar{t}_{\min}$ needs to be calculate based on Eq. (19). Using the obtained values for $\bar{t}$ and $t_{\min}$ from the previous section results in $\bar{t}_{\min} = 0.39$.

CH ($\bar{z}_c$) can be obtained by referring to Table 6 and selecting uniform load Case. Thus, the following equation should be used for calculating CH,

$$1.2529\bar{t}_{min}^{\,4} - 0.2699\bar{t}_{min}^{\,3} - 1.5707\bar{t}_{min}^{\,2} + 1.557\bar{t}_{min} + 0.0142 \tag{28}$$

Substituting $\bar{t}_{\min}$ in Eq. (28) results in $\bar{z}_c = 0.3955$. The other quantity that must be specified is $m(\bar{z})$. Based on Table 2 and the fact that uniform pattern is considered, $m(\bar{z}) = \bar{z}^{-2}$. Consequently, by substituting the obtained value of $\bar{z}_c$ and the equation of $m(\bar{z}) = \bar{z}^{-2}$ into relations (25), the thickness is evaluated, which its value in terms of *z* instead of $\bar{z}$ can be obtained by substituting z/h for $\bar{z}$. Doing so and considering *h*=120*m*, the final result for thickness is obtained as,

Region (*m*)	Thickness *t*(*z*) (*cm*)
$z \in [0 \quad 47.4]$	10
$z \in [47.4 \quad 120]$	$10\left(\frac{z}{47.4}\right)^2$

(29)

Dividing 47.4 by 3 (typical story height), results approximately 15 stories as the CS zone. Therefor the upper 15 stories (25-40 stories) have minimum value of thickness.

According to Eq. (29), *t*(*z*) is a continuously varying parameter. However, a continually varying thickness is not practical and further modification is required. In order to handle this issue, one can suppose that thickness would remain constant for every 5-levels (or 15-meters). The only constraint that must be observed while computing the equivalent thickness over a given 5-level span is to keep the material volume unchanged by selecting the average thickness over that span. At this point, all that remains is to calculate the dimensions of columns for each of the 5-story regions in accordance to their equivalent thickness value. This is done here using the relation $t = A_c / s$, and the results are presented in Table 8. Practical as well as theoretical values for column dimensions are also presented.

Table 8 Design information of example

Region (m)	Optimal thickness (cm)	Theoretical values of column dimensions (cm)	Practical values of column dimensions (cm)
0-45	10	50 ×50	50 ×50
45-60	12.99	56.99 ×56.99	55 ×55
60-75	21.38	73.11 ×73.11	75 ×75
75-90	31.9	89.29 ×89.29	90 ×90
90-105	44.51	105.49 ×105.49	100 ×100
105-120	59.23	121.69 ×121.69	120 ×120

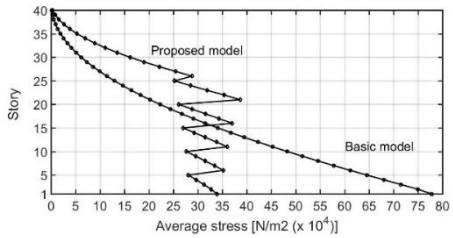

Fig. 7 Stress distribution along the height of basic and proposed structures

4.3 Software analysis and the results

Since the proposed method is based on bending deformation, it is expected that normal stresses due to bending would decrease in the proposed model, as compared to the reference model. Outputs from analyses using ETABS 9.7.4 (2011) reveal that the maximum axial stress in perimeter columns decreases by 47 percent. Hence, it validates the optimization process to some extent.

In order to get a better understanding of enhancements in the optimized structure, some new measures are introduced here, and the results are presented through a chart in Fig. 7. Data on the abscissa shows the average axial stress of compressed columns and the ordinate denotes the story number. Two graphs are drawn (reference and proposed models).

By a similar approach, three more parameters is defined; flange average stress: the average axial stress of compressed columns of the flange panels, web average stress: the average axial stress of compressed columns of the web panels, and maximum stress: the maximum axial stress of compressed columns,

From the diagrams in Fig. 7, it can be deduced that in addition to decrease in magnitude of normal stresses in the optimized structure, the stress field has a more uniform distribution. For a qualitative assessment of improvements to the new structure, two parameters are introduced in Table 9 for each parameter 1) Stress decrease: percentage decrease in Euclidean norm of (40-dimensional) the stress field, 2) Standard deviation decrease: percentage decrease in standard deviation of stresses as related to stories 1 through 25 (CC zone). The presented data in Table 9 confirm improvements in the proposed structure as compared to the reference structure,

Table 9 Stress and standard deviation along the height of structure

	Average stress	Flange Average stress	Web Average stress	Maximum stress
Stress decrease	27.74%	37.95%	17.11%	12.63%
Standard deviation decrease	82.64%	82.62%	82.20%	75.70%

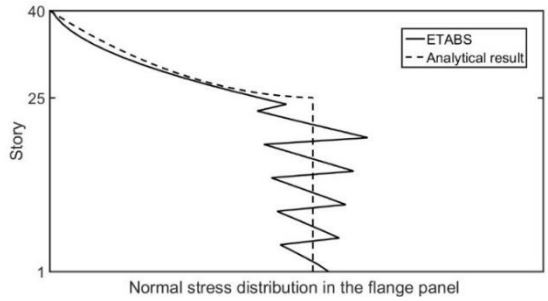

Fig. 8 Comparison of analytical and numerical results

in which the material is uniformly distributed along its height.

From Eq. (22) and using $m(\bar{z}) = \bar{z}^2$ from Table 2, it is anticipated that the curvature, and the normal stress as the result, varies by a polynomial of degree 2 in CT zone (25-40 stories); whereas, based on Eq. (23), stress distribution is uniform in CC zone (1-25 stories). These characteristics are illustrated in Fig. 8 by the dashed line. However, software analyses show that in the flange panel, the average of normal stress is distributed as the solid curve in Fig. 8. Clearly, there are some disparity between ETABS output and the analytical result, which can be attributed to the following approximations: a) in the analytic formulation (29), the thickness varies continuously, but in the ETABS model, due to some practical reasons, it is a piecewise function (Table 8). Therefore, there are some jumps in the ETABS diagram; b) the structural system used in ETABS is made up of some perimeter columns tied at each floor level by deep spandrel beams, whereas it is modelled by a simple tubular structure in the proposed method; c) the shear lag effect has been neglected in the analytic method, but it happens in the software modelling; d) the shear resistance of the structure is not taken into accounts in the approximate method.

5. Conclusions

In this study, a parametric-based method for optimal design of lateral stiffness in framed tube structures is presented; for which some practical constraints are considered. Important findings are as follows:

• Using variational calculus, a deformation profile is obtained as the optimality criterion, and the stiffness is then calculated based on this requirement.

• A constrained problem subjected to a lower bound limit was incorporated by dividing the design domain into two zones with specific characteristics; thereby allowing for derivation of the analytic relation.

• The obtained closed-form relation for stiffness may be used as a benchmark for numerical studies and for basic understanding of the framed tube structure behaviour. Furthermore, the proposed model is dimensionless; hence, it is applicable in any consistent unit system.

• The proposed method is based on bending deformation, so there is no guarantee that the methodology would lessen shear stresses. Nonetheless, since in tall-enough buildings, the dominant deformation is due to bending, the importance of shear stresses reduces as building's design height increases.

References

Aldwaik, M. and Adeli, H. (2014), "Advances in optimization of highrise building structures", *Struct. Multidisc. Optim.*, **50**(6), 899-919.

Bendsøe, M.P. and Sigmund, O. (2003), *Topology Optimization: Theory, Methods and Applications*, Springer, Berlin Heidelberg, New York, U.S.A.

Chan, C., Huang, M. and Kwok, K. (2010), "Integrated wind load analysis and stiffness optimization of tall buildings with 3D modes", *Eng. Struct.*, **32**(5), 1252-1261.

Christensen, P.W. and Klarbring, A. (2009), *An Introduction to Structural Optimization*, Springer Science, Business Media B.V.

Connor, J. and Laflamme, S. (2014), *Structural Motion Engineering*, Springer International Publishing, Switzerland.

Connor, J. and Pouangare, C. (1991), "Simple model for design of framed-tube structures", *J. Struct. Eng.*, **117**(12), 3623-3644.

Coull, A. and Ahmed, K. (1978), "Deflection of framed-tube structures", *J. Struct. Div.*, **104**(5), 857-862.

Coull, A. and Bose, B. (1975), "Simplified analysis of frame-tube structures", *J. Struct. Div.*, **101**(11), 2223-2240.

ETABS, Nonlinear Version 9.7.4 (2011), *Extended 3D Analysis of Building Systems*, Computer and structures Inc., Berkeley, U.S.A.

Jahanshahi, M.R. and Rahgozar, R. (2012), "Free vibration analysis of combined system with variable cross section in tall buildings", *Struct. Eng. Mech.*, **42**(5), 715-728.

Jayachandran, P. (2009), "Design of tall buildings: Preliminary design and optimization", *Proceedings of the International Conference on Tall Buildings and Industrial Structures*, Coimbatore, India, Keynote Lecture.

Kaviani, P., Rahgozar, R. and Saffari, R. (2008), "Approximate analysis of tall buildings using sandwich beam models with variable cross-section", *J. Struct. Des. Tall. Spec. Build.*, **17**(2), 401-418.

Khan, F.R. and Smith, S. (1976), "A simple method of analysis for deflection and stresses in wall-frame structures", *J. Build. Environ.*, **11**(1), 69-78.

Kwan, A. (1994), "Simple method for approximate analysis of framed tube structures", *J. Struct. Eng.*, **120**(4), 1221-1239.

Lee, S., Bobby, S., Spence, S., Tovar, A. and Kareem, A. (2012), "Shape and topology sculpting of tall buildings under aerodynamic loads", *Proceedings of the 20th Analysis and Computation Specialty Conference*, 323-334.

Liu, C. and Ma, K. (2017), "Calculation model of the lateral stiffness of high-rise diagrid tube structures based on the modular method", *Struct. Des. Tall. Spec. Build.*, **26**(4), e1333.

Mazinani, I., Jumaat, M.Z., Ismail, Z. and Chao, O.Z. (2014), "Comparison of shear lag in structural steel building with framed tube and braced tube", *Struct. Eng. Mech*s, **49**(3).

Montuori, G.M., Mele, E., Brandonisio, G. and Luca, A.D. (2014), "Design criteria for diagrid tall buildings: Stiffness versus strength", *Struct. Des. Tall. Spec. Build.*, **23**(17), 1294-1314.

Moon, K.S. (2010), "Stiffness-based design methodology for steel braced tube structures: A sustainable approach", *Eng. Struct.*, **32**(10), 3163-3170.

Moon, K.S. (2012), "Optimal configuration of structural systems

for tall buildings", *Proceedings of the 20th Analysis and Computation Specialty Conference*, 300-309.
Moon, K.S., Connor, J. and Fernandez, J. (2007), "Diagrid structural systems for tall buildings: Characteristics and methodology for preliminary design", *Struct. Des. Tall. Spec. Build.*, **16**(2), 205-230.
Rahgozar, R. and Malekinejad, M. (2012), "A simple analytic method for computing the natural frequencies and mode shapes of tall buildings", *J. Appl. Math. Model.*, **36**(8), 3419-3432.
Rahgozar, R., Ahmadi, A., Hosseini, O. and Malekinejad, M. (2011), "A simple mathematical model for static analysis of tall buildings with two outrigger-belt truss systems", *Struct. Eng. Mech.*, **40**(1), 65-84.
Smith, S. and Coull, A. (1996), *Tall Building Structures*, McGraw Hill Book Company, New York, U.S.A.
Stromberg, L.L., Beghini, A., Baker, W.F. and Paulino, G. (2011), "Application of layout and topology optimization using pattern gradation for the conceptual design of buildings", *Struct. Multidisc. Optim.*, **43**(2), 165-180.

CC